AN ACOUSTIC SENSOR ON THE SOLDIER MONITORS PHYSIOLOGY, VOICE, AND OTHER SOUNDS FOR SITUATIONAL AWARENESS

Michael V. Scanlon* and Latasha I. Solomon

US Army Research Laboratory
Sensors & Electron Devices Directorate, Adelphi, MD, 20783
mscanlon@arl.army.mil and lsolomon@arl.army.mil

ABSTRACT

Acoustic sensors on the future warriors will be able to not only detect tactical target signatures for enhanced situational awareness, but they will also be able to monitor the health, performance, and voice of the soldiers wearing these sensors. This use of this information is crucial for soldier survivability, lethality, and mobility. The Army Research Laboratory (ARL) has developed a unique body-contacting acoustic sensor that can monitor the health and performance of soldiers or firefighters while they are doing their mission. ARL has put sensors on soldiers and firefighters to monitor them. Vital-sign indications and physiological parameter trends of soldier in strenuous and hazardous environments can be continuously and remotely monitored. Very diverse physiological indicators can be detected with acoustic sensors.

1. INTRODUCTION

Since the Objective Force Warrior will require a communications sensor, judicious selection of a single sensor that detects voice, physiology and other acoustic events will eliminate redundant sensors and reduce the weight, power, and cube of future soldier ensembles. The ARL has developed a unique body-contacting acoustic sensor that can monitor the health and performance of soldiers or firefighters while they are doing their mission [Scanlon, 1998]. ARL's unique gel-coupled sensor has acoustic impedance properties similar to the skin that facilitate the transmission of body sounds into the sensor pad, yet significantly repel ambient airborne noises due to an impedance mismatch. ARL's emphasis has been to put sensors on soldiers to monitor them while they are doing their mission. Vital-sign indications and physiological parameter trends of soldier in strenuous and hazardous environments can be continuously and remotely monitored with acoustic sensors. The acoustic physiological sensor data can augment other medical monitoring initiatives, and can contribute important information to other larger Army programs such as Land Warrior, Scorpion, Objective Force Warrior, Warfighter Physiological Status Monitor, Warrior Medic, and Future Combat System of Systems. The patented technology will benefit the commercial sector for ambulatory health monitoring and can be purchased for research purposes from Sensory Devices in New Eagle, PA [Scanlon, 1996].

2. EXPERIMENT AND HARDWARE

ARL conducted an experiment at the University of West Virginia's Firefighter Training Academy in Morgantown, WV [Scanlon, 2002]. Firefighters from the Clarksburg fire department volunteered to be monitored during their normal training in the burning building facility. Two scenarios were developed for the experiment. The first experiment, which will be termed the smoke-test, required the firefighting team to crawl/walk through a smoke-filled two-story building with an uncharged 1.5-inch hose to search for and rescue a mannequin (located on the second floor). Once the mannequin was brought down the stairs and outside, the firefighters then went back to where they found the mannequin and brought the hose back out. Burning hay in a 55-gallon drum created the smoke. The second experiment, termed the fire-test, required the firefighters to enter a smoke-filled building to locate a disoriented firefighter on the first floor whose alarm was sounding, escort him to safety, then proceed upstairs to put out the fire with the 1.5 inch hose. Burning several pallets and wood pieces created the fire and smoke. The purpose of this test was to see how well the acoustic sensors monitored physiology amidst the intense activity and environment. Data was collected for post-processing. Sensors, data acquisition hardware, and data transmitter were attached to one firefighter, who was the lead of the team and was at the nozzle of the hose. Digitized data was stored on a small body-worn computer as well as digitally transmitted to another laptop in a safe location. The equipment used on this test allowed for redundancy of acoustic sensors and data acquisition, but would not be present for a fielded system. In addition to the acoustic sensors, electrocardiogram (ECG) sensors were used to verify the heart rate, temperature sensors quantified the thermal ambient environment, and a microphone characterized the ambient noise.

Figures 1 and 2 show the gel-coupled neck acoustic sensors and it's positioning in this test below the hood. Two sensors were chosen for redundancy and noise canceling features. Heartbeats, breaths, and voice all appear simultaneously at the two sensors, but motion artifacts may be out of sync and different in signature. Figures 3 and 4 show how the mask acoustic sensor is attached. Although Velcro was a field expedient solution in this test, the sensor could ultimately be build into the helmet, hood, or mask itself for similar contact. An

acoustic sensor in the mask position picks up heartbeat pulses from the temple, breath sounds through sinus and tissue conduction, voice, coughing, wheezes, and activity.

Fig. 1: Neck sensor strap   Fig. 2: Sensor on neck
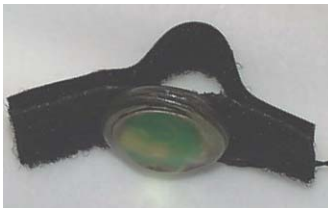
Fig. 3: Mask sensor   Fig.4: Sensor on mask

Figures 5 and 6 show the wrist acoustic sensors in a wristband embodiment. In proximity to the sensor were positioning mechanisms to ensure the band did not rotate, and kept the sensor over the radial artery for strongest signal positioning. Figure 7 also shows the seven-lead (three channel) ECG pads and wires, along with a commercially available Polar Heart Monitor chest band often used by runners. The firefighter's jacket in figure 8 protects the equipment while the firefighter is being monitored. The three-channel ECG data is stored on the Holter Monitor's PCMCIA memory card. The 1st channel of the ECG is also fed into the computer's data acquisition card. Not shown is the Holter monitor, transmitter, boom microphone, temperature probe, BioRadio data transmitter, and the PCMCIA eight-channel data acquisition card that goes into the Libretto hand-held computer. Underneath the computer is the preamplifier and anti-aliasing filter for each sensor prior to digitization by the DAQ-card.

Fig. 5:Wrist sensors   Fig. 6: Sensor on wrist

Fig. 7: ECG/Polar   Fig. 8: Full gear

3. DATA AND RESULTS

ECG derived heart rate was collected for both firefighters doing both scenarios. Firefighter number one reached an average heart rate of 165 beats per minute (BPM) while dragging the mannequin to safety, whereas he only reached 152 BPM while putting out the fire. Firefighter number two reached an instantaneous maximum heart rate of 182 BPM while maneuvering the mannequin in the smoke-test, and 168 BPM during the fire-test. The data also showed that firefighter number two's resting heart rate (between smoke and fire events) stayed near 110 BPM, whereas firefighter number two was able to get below 100 BPM during the rest period. Prior to the first test, both firefighters' heart rates were approximately 80 BPM. The ability to monitor this resting heart rate, when the physiological signal-to-noise ratio (SNR) is good, is in itself is an important tool, in that it can be a indicator of which firefighters are ready to reenter a building fire or need to be relieved. The duration of elevated heart rates and the maximum rate achieved can also be an indicator of a firefighter's ability to safely perform his or her mission.

Alternating wrist activity was present often in these scenarios, and is indicative of the firefighter crawling on the floor (the jarring motion artifacts from using alternating hands to support him as he crawled). Very often the amplitude of the intense activity exceeded the maximum input range for the data acquisition and was clipped. By using a 16- or 24-bit A/D converter, instead of the 12-bit used in this test, clipping would no longer occur. Although clipping of the data is undesirable from a data processing point of view, it does indicate that the firefighter is still active and involved in some form of intense motion. In its simplest form, one might conclude that if he is still moving, he is still healthy, regardless of whether the physiology is visible amongst motion artifacts.   The heartbeats from the acoustic mask sensor are clearly visible at the beginning of this set, but are less apparent when the crawling activity starts. The mask physiology is often lost due to firefighters constantly turning their heads while maneuvering, and resulting motion of the breathing hose, mask, and helmet were transmitted through the mask straps to the sensor. The SNR of the heartbeat physiology at the head is not a strong as at the neck. The ECG suffers from motion artifacts during the intense motion sections.

The data shows very clear acoustic heart signals with distinct peaks for determining the inner-beat-intervals (IBI's). For example, a person with a short-time average heart rate of 60 BPM might have ten beats spaced exactly 1-second apart, or five beats slightly above and five beats slightly below 1-second intervals, with an irregular IBI sequence during that 10-second period. How the IBI's fluctuate on a beat-by-beat basis, as well as long-term trends, is termed heart rate variability (HRV) and gives an indication of how well the body is regulating blood pressure, breathing, and core temperature [Mulder, 1981]. These IBI's also can indicate mental activity related to concentration on a task, or varying due to mental and physical distractions.

Figure 9 shows two seconds of data from the computer-based storage. From top to bottom the sensors are: L-neck, R-neck, L-wrist, R-wrist, ambient microphone, mask, polar HR, and ECG. Note the very clear indications of heartbeats on all physiological sensors. Of significant importance is the time-difference-of-arrival between the ECG and the neck and wrist acoustic pulses. The literature shows that changes in the pulse-wave-velocity (PWV) are directly proportional to changes in the systolic blood pressure [Dauzat, 1996]. The ECG monitors the electrical stimulus that creates a mechanical pressure wave that leaves the heart and travels through the arteries. The time it takes for the pulse to travel between two fixed locations (such as from the heart to the wrist) is directly proportional to the pressure of the blood (speed of sound in the artery changes with respect to density and the velocity component of the blood flow). By measuring the time-difference between the heartbeat indications from ECG-neck, ECG-wrist, ECG-head, neck-wrist, head-wrist, and neck-head, one can approximate the systolic blood pressure on a beat-by-beat basis. The neck and wrist acoustic sensors provide the largest length of travel (and delta-time), and therefore would permit best timing resolution with the lower sample-rates of wearable data acquisition systems.
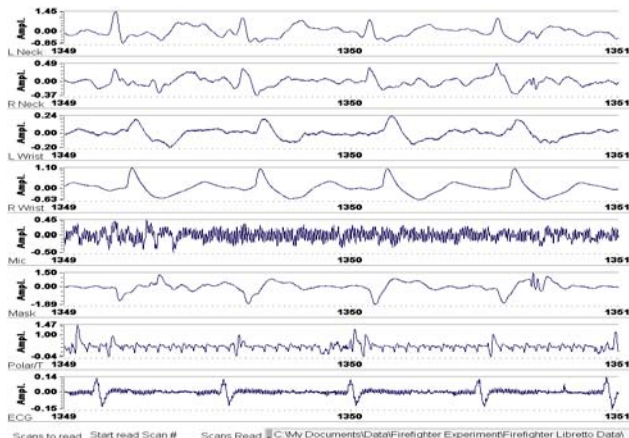
Cross-correlation techniques between the wrist and neck acoustic sensor bring out the PWV time shift very well [Scanlon, 2001]. Note that the time-differences between the ECG waveforms and Polar heartbeat indications are a result of the Polar processor, transmitter, and receiver delays.

The acoustic sensors and transmitters used in this experiment could have been built into a wristwatch and helmet headband, and provide the same data without the firefighter even knowing he or she is being monitored. The wristwatch alone could be worn continuously to monitor pre- and post-alarm heart rate, and activity. Work has been done in approximating systolic pressure from the slope of the second heart-sound, but it is not as accurate as the PWV technique since there are many physiological variables that also affect the pulse shape [Bartles, 1992]. It is also possible that breath rates can be derived from acoustic pulses at the wrist by analyzing changes in amplitude that result from the lungs over- or under-pressurizing the heart. This phenomenon of decrease in pulse pressure during inspiration is called "pulsus-paradoxis", and is often associated with situations where respiration is labored [Parsons, 1978].

As mentioned earlier, ARL's gel-coupled sensor is excellent for voice reception. Figure 10 compares the neck-acoustic sensor (top) to the boom microphone (bottom) during speech. Both sensors detect intelligible speech, but the ambient noise rejection of the neck-contacting sensor is excellent and the voice SNR is higher with the neck acoustic sensor. The gel-coupled neck sensor has demonstrated significant SNR benefits over boom microphones for use with automatic speech recognition software such as Entropic, ViaVoice, and Dragon Naturally Speaking [Bass, 1999].
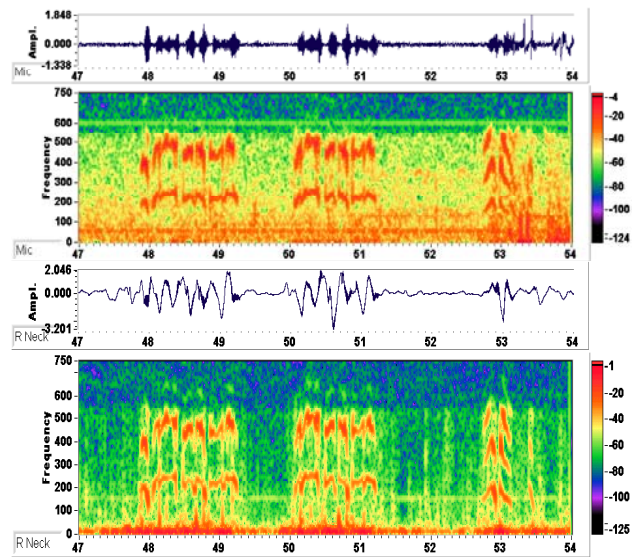
Fig. 10: Spectrogram comparing voice at airborne mic (top) and gel-sensor on neck (bottom)

Fig. 9: Two seconds of computer stored physiology

Figures 11, 12, and 13 show time series and spectrograms of 80-seconds of data during a simulated unconscious firefighter. The first 20-seconds show him walking, standing, and then getting into position on the ground. He then holds as still as possible for approximately 40-seconds until his motion sensor alarm activates, then he gets up off of the ground. Figure 11 shows excellent heartbeats and breaths in the middle section with minimal motion artifacts. Figure 12 shows an increase in the amplitude of the neck heart sound, resulting either from more blood flow from being in the horizontal prone position, or because coupling pressure increased because of a change in neck band position or tension. Breath sounds are clearly visible throughout. Figure 13 shows wrist acoustic activity getting into position on the ground, excellent pulsations throughout the unconscious period, and intense wrist activity to get up at the end of the scenario.
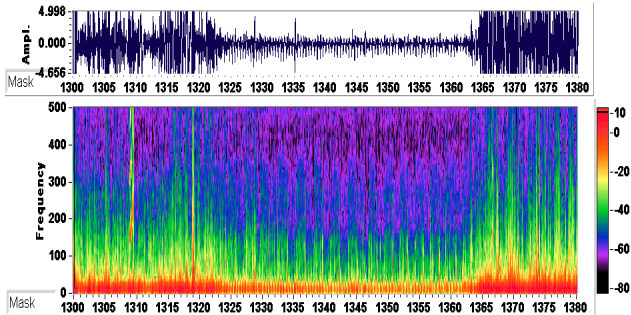
Fig. 11: Spectrogram and time-series of mask data during unconscious scenario
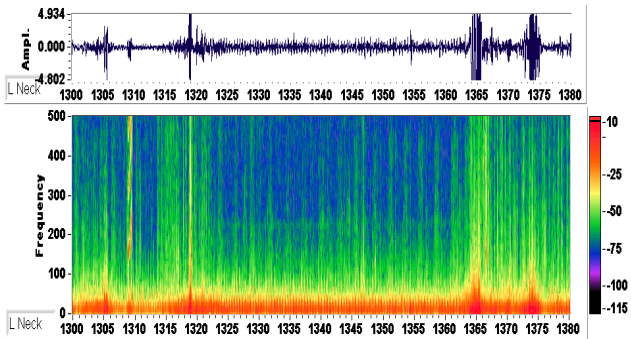
Fig. 12: Spectrogram and time-series of L-neck data during unconscious scenario
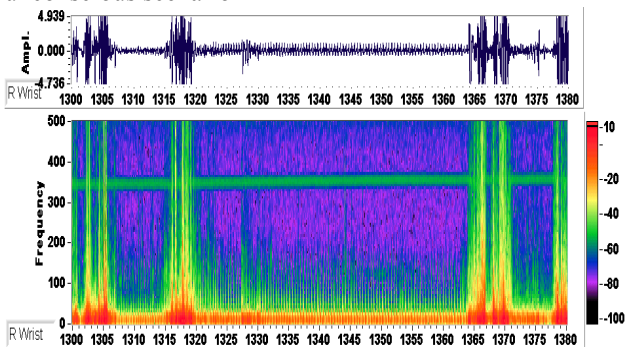
Fig. 13: Spectrogram and time-series of R-wrist data during unconscious scenario

4. SIGNAL PROCESSING

One method to monitor the firefighters is to look at short-term energy detected at the sensors. The higher the RMS energy is the higher the activity. Figure 14 shows RMS calculations on the wrist sensor data during the smoke-test. Figure 14 indicates when the firefighter was crawling, maneuvering the mannequin for extraction, and retrieving the hose after the mannequin was removed. Had the high-level activity diminished significantly for a significant period, it would be readily apparent, and could cause an alert to be sent, much like the firefighter's PAS motion sensor already does. High levels at the neck result from head turns, voice, jacket, hood, mask movements, and muscular activity from lifting or crawling.
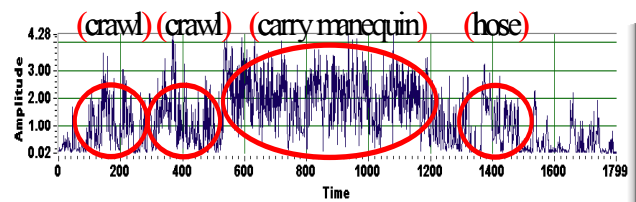
Fig. 14: RMS energy of left wrist sensor (30 minutes)

When a firefighter goes down due to injury, the SNR of the physiology improves greatly. This is when medical monitoring is needed most. The decrease in RMS energy at all acoustic sensors will indicate a decrease in activity.

One advanced signal processing technique used to discern physiology from noise is the normalized Lomb-Scargle (L-S) periodogram. This research compares and contrasts the short-time Fourier transform (STFT) with the Lomb-Scargle (L-S) normalized periodogram. Both algorithms were applied to the neck and wrist acoustic signal in an attempt to extract the subject's heart rate in "real-time". The L-S periodogram was initially given preference over other spectrum analysis techniques because previous research has proven that it produces excellent results when processing non-stationary, unevenly occurring features [Whitney and Solomon, 2001].

Classical spectrum analysis methods for quantifying periodicities, such as the Fast Fourier Transform (FFT) assume that the data to be processed is sampled periodically and stationary such that it's statistical characteristics do not change with time. However most biomedical signals are not stationary and posses complex time-frequency characteristics. The short time Fourier Transform (STFT) attempts to satisfy the conditions of stationarity by dividing the signal into blocks of short segments in which the signal can be assumed to be stationary. The problem with the STFT is choosing an optimal window processing length. If the analysis window chosen is too short, the resulting frequency resolution may be poor. Choosing a longer window will increase

frequency resolution, however the assumption of stationarity within the window is compromised.

The Lomb-Scargle normalized periodogram evaluates data only at times, *t(j),* that are actually measured and is defined in Equation 1 as

$$P(\omega) \equiv \frac{1}{2\sigma^2} \left\{ \frac{\left[\sum_{j=1}^{N}(x(j)-\bar{x})\cos\omega(t(j)-\tau) \right]^2}{\sum_{j=1}^{N}\cos^2\omega(t(j)-\tau)} + \frac{\left[\sum_{j=1}^{N}(x(j)-\bar{x})\sin\omega(t(j)-\tau) \right]^2}{\sum_{j=1}^{N}\sin^2\omega(t(j)-\tau)} \right\}$$

(1)

where *x(j)* is the input data, *N* is the length of the input data, $\omega \equiv 2\pi f$, and the offset τ is defined in Equation 2 as

$$\tau = \left(\frac{1}{2\omega} \right) * \tan^{-1} \left(\frac{\sum_{j=1}^{N}\sin 2\omega t(j)}{\sum_{j=1}^{N}\cos 2\omega t(j)} \right)$$

(2)

making *P(ω)* independent of any time shift. The advantage of L-S algorithm is that it weights the data on a "per point" basis instead of a "per time interval" basis [Press, 1992].

An individual's heart rate can vary drastically over a 30-minute time interval. After testing several window lengths, a 5 second or 7500 sample duration was chosen as the processing window length with a 95% overlap. This window length produced optimal results because it contained an adequate amount of data points needed to produce a meaningful heart rate spectrum, however it was not too long whereby causing spurious peaks in the spectrum relating to heart rate variability during those periods of transition for walk to run cycles. To eliminate DC offset, the bias was subtracted from the windowed signal. Next, a 40 Hz low pass filter was applied to the neck acoustic data, and a 20 Hz low-pass filter was applied to the wrist data. To expedite the processing time, the data was decimated by a factor of 10, thus making *N* equal to 750 samples. Finally, both a 4096-point STFT and the Lomb-Scargle periodogram were applied to the decimated signal and the time-frequency spectrum was computed. The L-S periodogram analyzed the data at 798 independent frequencies, *f*, from 0-40 Hz. The number of independent frequencies was derived from the following equation:

$$f = \left(\frac{ofac * N}{2} \right) \left(\frac{f_{hi}}{N/2T} \right)$$

(3)

where *ofac*, the oversampling parameter, is set equal to 4 based on previous research [Press, 1992], f_{hi} is 40Hz, and *T* which is the time difference between maximum and minimum data points to be analyzed is equal to approximately 5 sec.

Figures 15 and 16 illustrate the unprocessed signal extracted from the right wrist and left neck acoustic sensors. This interval captures approximately 80 seconds of physiological data where the individual pretended to be unconscious. During the first portion of the data the subject is positioning himself to lie down, followed by the unconscious scenario, and finally he gets up to walk away after being rescued.
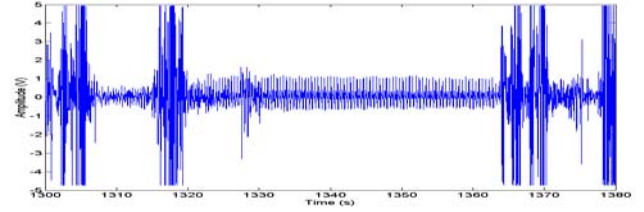
Fig. 15: Right wrist acoustic data.
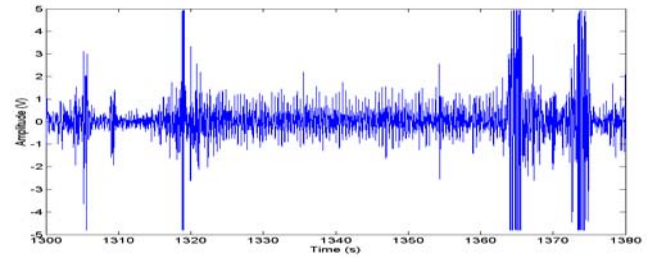
Fig. 16: Left neck acoustic data.

Figures 17 and 18 illustrate the spectrogram of the right wrist and left neck acoustic sensor data respectively. Analysis of the graphs indicates that the STFT produces a good estimation of the fundamental heart rate frequency and its corresponding harmonics even though the processed data is not stationary.
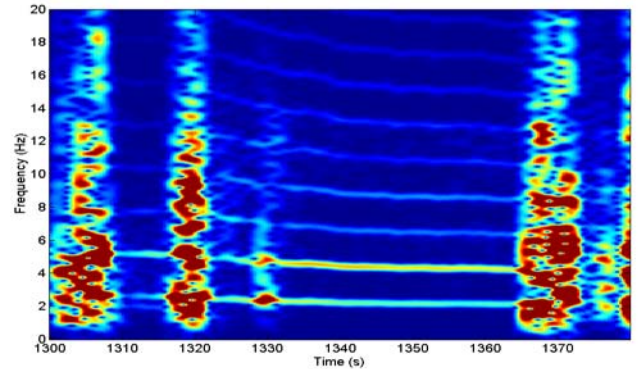
Fig. 17: STFT of right wrist acoustic data.
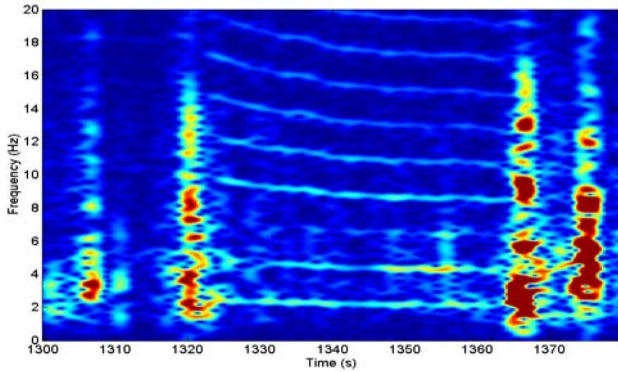
Fig. 18: STFT of left neck acoustic data.

Figures 19 and 20 illustrate the results obtained after the L-S periodogram was applied to the same data set as mentioned above. One will notice that the L-S produces improved time-frequency resolution as compared to that of the STFT.
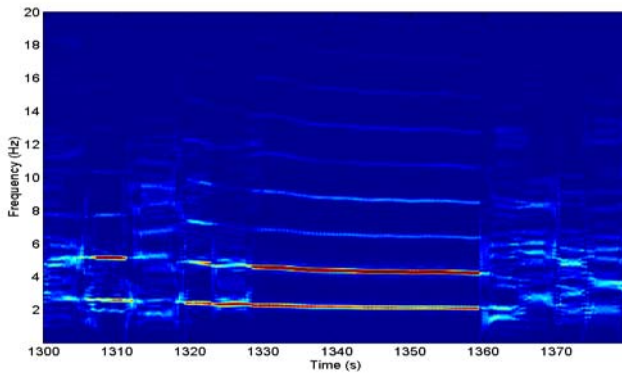
Fig. 19: L-S results of right wrist acoustic data.
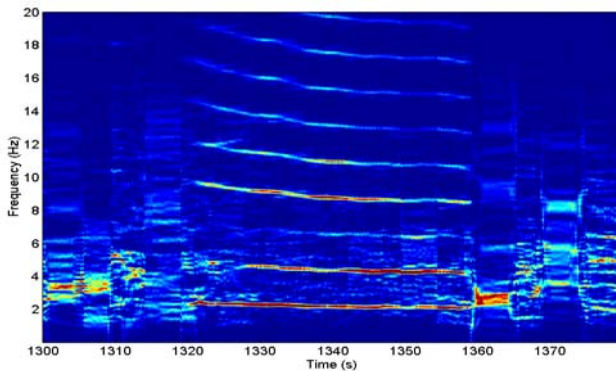
Fig. 20: L-S results of neck acoustic data.

Analysis of the above results indicates that both acoustic sensors produce excellent results in heart rate extraction ($\approx$ 2.8 Hz) during those periods of low-level activity. However, when the sensors are subjected to intense motion activity, the desired physiological signal is distorted due to motion artifacts caused by muscle movement and the jarring of sensors against the body. It is during those intervals that the calculated periodogram serves as very little help in detecting heart rate. It should

also be noted that the noise experienced by the wrist acoustic sensor varies in some instances with that of the neck acoustic sensor therefore if one set of data experiences noise due to motion artifact one may very well be able to extract the soldier's vital signs from an acoustical sensor placed at another body location.

A harmonic line analysis algorithm was then applied to the data. The trend for producing the heart rate or fundamental frequency is a result of the fact that a periodic signal having period τ also exhibits the periods 2τ, 3τ, etc., and the residual error obtained by fitting a noise corrupted signal by a periodic signal with minimal periodicity τ decreases with increasing τ [Dommermuth, 1993]. Normally, the heart beats at a steady 60 to 80 beats/minute or 1-1.3 Hz, respectively.   However during intense exercise, ones heart rate may increase up to 200 (3.3 Hz) or more beats/minute. Based on this information, only those fundamental frequencies located between 0.9 and 3.3 Hz are accepted as valid heart rate estimations. The estimated heart rate was then computed by setting it equal to the fundamental frequency that contained the largest number of harmonics. If by chance the algorithm found no frequencies within the specified interval the heart rate was set equal to zero.

Figure 21 through 24 illustrate the harmonic line analysis results of both the wrist and neck acoustic signal. The heart rate estimate is plotted against the STFT of the polar heart monitor data in figures 21 and 22 as opposed to the L-S periodogram of the polar data in figures 23 and 24. The polar heart monitor data was considered to be the "truth data" as opposed to the ECG signal during this same interval due to the amount of distortion experienced during those times of activity. The ECG leads were not adequately applied to the chest area, thus permitting motion artifacts to obscure the desired physiology during moderate activity.
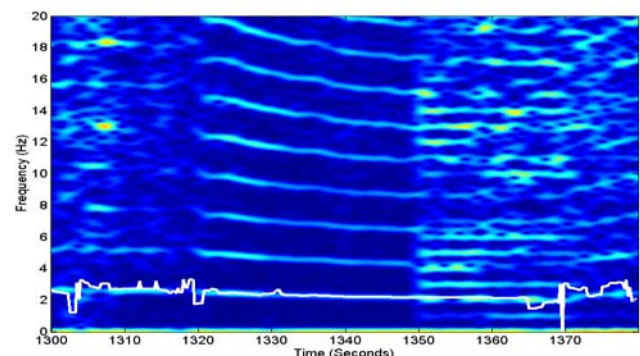
Fig. 21: Right wrist heart rate estimation plotted against STFT of the polar data.
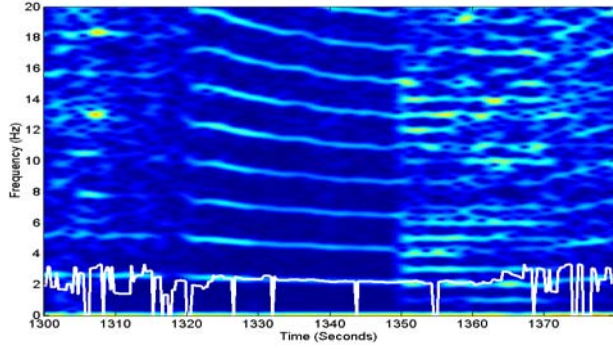
Fig. 22: Left neck heart rate estimation plotted against STFT of the polar data.
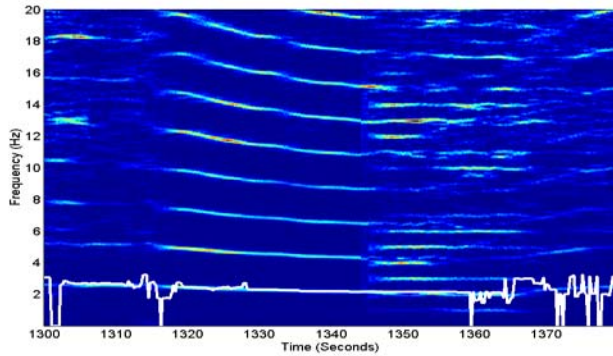
Fig. 23: Right wrist heart rate estimation plotted against L-S periodogram of polar data.
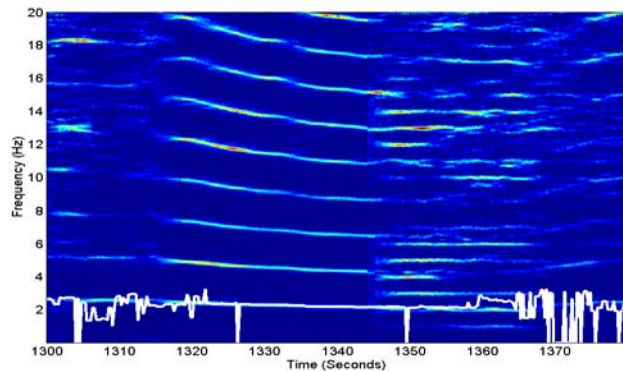
Fig. 24: Left neck heart rate estimation plotted against L-S periodogram of polar data.

In general, the harmonic line analysis algorithm performs equally as well when applied to both the STFT and the L-S of the wrist acoustic data. However, when applying the harmonic line analysis algorithm to neck acoustic data, the results obtained using the Lomb-Scargle periodogram are an improvement as compared to those using the short-time Fourier transform. Smoothing algorithms can be implemented to reduce the noise-induced variations from the actual heartbeat frequency.

As a simple example of breath rate detection, high-passed neck data reveals a lot of broadband high-frequency energy resulting from the airflow in the throat. Using fast-Fourier transforms (FFT's) to monitor the temporal fluctuations of the RMS energy produces a breath rate peak in the power-spectrum results. Figure 25 shows intentionally clipped time-series data from the neck sensor, and the resulting half-second sliding window RMS energy. The clipping of the data removes the influence high-amplitude motion artifacts have on the RMS calculation, and was clipped at a level of three times the median value of the absolute value of the band-pass filtered data. The band-passed spectrogram of figure 25 also shows the broadband breath cycles. At the bottom of figure 25 is the power spectrum of the RMS energy for the 24-seconds shown. The 0.45-Hz breath rate represents a breath every 2.2 seconds, which is supported by the ten breath-cycles seen in the 24-seconds of data. Data from the mask sensor showed the strongest signal was also at 0.45-Hz.
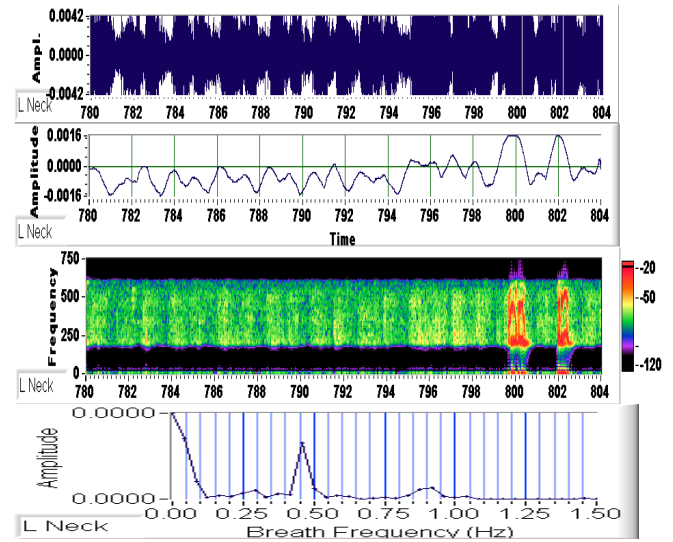
Fig. 25: Time, RMS, band-passed spectrogram of L-neck, result by FFT breath rate extraction from RMS data

5. DISCUSSION

This research proves that Lomb-Scargle normalized periodogram serves as an excellent tool for heart rate extraction from acoustic sensors when there exists a high signal-to-noise ratio and very little motion artifact. It can also be concluded that the short-time Fourier transform produces an acceptable estimate of heart rate even though this algorithm is most commonly used to process stationary data. In an attempt to improve upon this algorithm, the root mean square (RMS) energy can be calculated and used as a reference to indicate the soldier's level of activity. If the monitored soldier's energy exceeds a certain threshold it can be assumed that the soldier is active and well, and the predicted heart rate value may be discarded. However, during periods of low-level activity the soldier's vital signs are of most importance and should be monitored continuously. If the RMS energy is low this may very well be an indication that the soldier is wounded and in need of medical attention.

6. CONCLUSION

Acoustic sensors and signal processing can extract much information about the firefighters health and performance. Transmitted data shows that heart rate, breath rate, blood pressure and activity can be monitored by medics/commanders at a remote location. The quality of the acoustic data is excellent, and can provide much more information than the ECG. The Lomb-Scargle periodogram and RMS energy processing of acoustic sensor data provides excellent measures of heart rate and motion activity. Breath rates are measured from high-frequency broadband sounds at the neck or mask or pulse amplitude variations at the wrist. Timing (PWV) between two sensors indicates systolic blood pressure on a beat-by-beat basis. The IBI's give pulse rate and an indication of heart rate variability. The acoustic data from this test demonstrates that even though physiology is sometimes masked by motion and activity artifacts, is still provides useful indicators that the firefighter is still active and most likely functioning effectively. It is when the person being monitored ceases to be active or during resting periods that the acoustic SNR is exceptional for monitoring physiology. This is when vital signs monitoring is most important. Acoustic sensors and a transmitter will be incorporated into a garment, which will reduce some of the motion artifacts resulting from the cables and data logging equipment. It is felt that such a shirt could be worn continuously while firefighters are on call to monitor the stressful and demanding nature of their entire shift. The same shirt will be evaluated on soldiers and for home health monitoring. Very diverse physiology is detectable with a single acoustic sensor, and more information provides a better situational understanding of how the soldier is being effected by the environment, equipment, and mission.

REFERENCES

Bartels, A., and D. Harder, "Non-invasive determination of systolic blood pressure by heart sound pattern analysis," Clinical Phys. Physiol. Meas., Aug. 1992; 13(3): pp. 249-256.

Bass, James D, Scanlon, Michael V., Morgan, John J, "Getting Two Birds with One Phone: An Acoustic Sensor for Both Speech Recognition and Medical Monitoring", 138th Meeting of the Acoustical Society of America, Columbus, Ohio, 2 Nov. 1999.

Dauzat, M., Deklunder, G., Adam, B., de Cesare, A., Ayoub, J., Masse-Biron, J., Prefaut, C. Peronneau, P., "Pulse Wave Velocity Measurement by Cross-Correlation of Doppler Velocity Signals. Application to Elderly Volunteers During Training", Int. J. Sports Med., 1996, Nov.; 17(8): 547-53.

Dommermuth, F.M., *Estimation of Fundamental Harmonics*, IEE Proceedings-F, Vol. 140, No. 3, pp. 162-170, 1993.

Mulder, G. and L. J. M. Mulder, "Information Processing and Cardiovascular Control", Psychophysiology, 1981, 18: pp. 392-405.

Parsons, G. and J.F. Green, "Mechanisms of pulsus paradoxis in upper airway obstruction," J. Appl. Physiology., 45:598-603, 1978.

Press, William, *Spectrum Analysis of Unevenly Sampled Data*, Numerical Recipes In C. Cambridge University Press, NY, p.575-584, 1992.

Scanlon, M. V., *Sudden infant death syndrome (SIDS) monitor and stimulator*, May 1996, U.S. Patent 5,515,865; *Motion and sound monitor and stimulator*, Nov. 4, 1997, U.S. Patent 5,684,460; *Acoustic monitoring sensor*, Dec. 29, 1998, 5,853,005. ARL patents non-exclusively licensed for "manufacture and sell for research purposes only" by Sensory Devices, 205 Main Street, New Eagle, PA, 15067, (724) 258-5353.

Scanlon, Michael V., "Acoustic Sensor for Health Status Monitoring", Proceedings, IRIS Acoustic and Seismic Sensing, 1998, Volume II, pp. 205-222.

Scanlon M., "Acoustic sensor extract physiology during activity", 17th Int'l Congress on Acoustics, Sept. 6, 2001, Rome, Italy.

Scanlon, M. V., Proc. of SPIE's 16th Int'l AeroSense, 5 April 2002, Orlando, FL, #4708-86 "Acoustic Monitoring of First Responder's Physiology for Health and Performance Surveillance". (www.arl.army.mil/acoustics/michael_scanlon.htm)

Whitney, James, and Latasha Solomon, Respiration Rate Signal Extraction from Heart Rate, Proceedings of SPIE Vol. #4368 Visualization of Temporal and Spatial Data for Civilian and Defense Applications III, p.104-112, April 2001.